

# Discontinuous Non-Rigid Motion Analysis of Sea Ice using C-Band Synthetic Aperture Radar Satellite Imagery

Mani Thomas  
Video/Image Modeling and Synthesis Lab  
University of Delaware  
Newark, Delaware  
manivt@cis.udel.edu

Cathleen Geiger  
Snow and Ice Branch  
USACRREL  
72 Lyme Rd, Hanover, NH 03755  
cathleen.a.geiger@erdc.usace.army.mil

Chandra Kambhamettu  
Video/Image Modeling and Synthesis Lab  
University of Delaware  
Newark, Delaware  
chandra@cis.udel.edu

## Abstract

*Sea-ice motion consists of complex non-rigid motions involving continuous, piece-wise continuous and discrete particle motion. Techniques for estimating non-rigid motion of sea ice from pairs of satellite images (generally spaced three days apart) are still in the developmental stages. For interior Arctic and Antarctic pack ice, the continuum assumption begins to fail below the 5 km scale with evidence of discontinuities already revealed in models and remote sensing products in the form of abrupt changes in magnitude and direction of the differential velocity. Using a hierarchical multi-scale phase-correlation method and profiting from known limitations of cross correlation methods, we incorporate the identification of discontinuities into our motion estimation algorithm, thereby descending below the continuum threshold to examine the phenomenon of discontinuous non-rigid sea-ice motion.*

## 1. Introduction

Sea-ice consists of a collection of floes<sup>1</sup> with differential motion subject to non-local forcing at an aggregate-scale with ranges from 10-300 km spatially and 1-20 days temporally [37], [34]. This differential motion results in features such as leads, families of slip lines, cracks, and ridges. Within the sea-ice community there is no formal definition of this scale. Coon, et al. [14], Aksenov and Hibler [1],

and Wilchinsky and Feltham [42] have made progress in developing theoretical “anisotropic” sea-ice rheologies, but adequate data products to rigorously test their theories do not exist. Within the literature definitions of discontinuous behavior such as “linear kinematic features” (LKF) [27], [35], “piece-wise rigid motion” [35] and “aggregate scale” [23], [37] are beginning to emerge. The fundamental problem in defining these features is that their composition transcends any one scale, with several scales embedded upon one another.

Fundamentally, aggregate-scale sea ice is a piece-wise continuous material made up of a collection of aggregated plates subject to the basic principles of continuum mechanics with limitations of those basic principles in close proximity to discontinuities. This definition places the motion of sea ice under the larger category of non-rigid motion analysis [26]. The interdisciplinary field of non-rigid motion involves the understanding of three basic types of materials, namely, continuous, piece-wise continuous, and discrete particle motion. Depending on the scale, each of these descriptions applies to sea ice. At the large (basin) scale, sea ice is traditionally regarded as a non-rigid continuum and at the small scale it is regarded as a collection of discrete particles/floes.

While progress has been made in understanding these two outer scales of sea ice, the intermediate scale of piece-wise continuous sea-ice motion is particularly difficult because it goes beyond the limits of its scale with very narrow (i.e., small scale) crack-like features stretching thousands of kilometers (i.e., basin scale). This scale is one which researchers have only recently been able to explore thanks to

---

<sup>1</sup> A single piece, large or small, of ice formed on the surface of an ocean or sea.

Report Documentation Page			Form Approved OMB No. 0704-0188		
Public reporting burden for the collection of information is estimated to average 1 hour per response, including the time for reviewing instructions, searching existing data sources, gathering and maintaining the data needed, and completing and reviewing the collection of information. Send comments regarding this burden estimate or any other aspect of this collection of information, including suggestions for reducing this burden, to Washington Headquarters Services, Directorate for Information Operations and Reports, 1215 Jefferson Davis Highway, Suite 1204, Arlington VA 22202-4302. Respondents should be aware that notwithstanding any other provision of law, no person shall be subject to a penalty for failing to comply with a collection of information if it does not display a currently valid OMB control number.					
1. REPORT DATE <b>27 JUN 2004</b>		2. REPORT TYPE		3. DATES COVERED -	
4. TITLE AND SUBTITLE <b>Discontinuous Non-Rigid Motion Analysis of Sea Ice using C-Band Synthetic Aperture Radar Satellite Imagery</b>				5a. CONTRACT NUMBER	
				5b. GRANT NUMBER	
				5c. PROGRAM ELEMENT NUMBER	
6. AUTHOR(S)				5d. PROJECT NUMBER	
				5e. TASK NUMBER	
				5f. WORK UNIT NUMBER	
7. PERFORMING ORGANIZATION NAME(S) AND ADDRESS(ES) <b>USACE Engineer Research and Development Center,Cold Regions Research and Engineering Laboratory,72 Lyme Road,Hanover,NH,03755-1290</b>				8. PERFORMING ORGANIZATION REPORT NUMBER	
9. SPONSORING/MONITORING AGENCY NAME(S) AND ADDRESS(ES)				10. SPONSOR/MONITOR'S ACRONYM(S)	
				11. SPONSOR/MONITOR'S REPORT NUMBER(S)	
12. DISTRIBUTION/AVAILABILITY STATEMENT <b>Approved for public release; distribution unlimited</b>					
13. SUPPLEMENTARY NOTES <b>The original document contains color images.</b>					
14. ABSTRACT <b>Sea-ice motion consists of complex non-rigid motions involving continuous, piece-wise continuous and discrete particle motion. Techniques for estimating non-rigid motion of sea ice from pairs of satellite images (generally spaced three days apart) are still in the developmental stages. For interior Arctic and Antarctic pack ice, the continuum assumption begins to fail below the 5 km scale with evidence of discontinuities already revealed in models and remote sensing products in the form of abrupt changes in magnitude and direction of the differential velocity. Using a hierarchical multi-scale phase-correlation method and profiting from known limitations of cross correlation methods we incorporate the identification of discontinuities into our motion estimation algorithm, thereby descending below the continuum threshold to examine the phenomenon of discontinuous non-rigid sea-ice motion.</b>					
15. SUBJECT TERMS					
16. SECURITY CLASSIFICATION OF:			17. LIMITATION OF ABSTRACT	18. NUMBER OF PAGES <b>9</b>	19a. NAME OF RESPONSIBLE PERSON
a. REPORT <b>unclassified</b>	b. ABSTRACT <b>unclassified</b>	c. THIS PAGE <b>unclassified</b>			

the availability of high-spatial resolution, all-weather Synthetic Aperture Radar (SAR) images [15], [16], [17], [19]. This paper delves into the estimation and validation of sea-ice motion using SAR images from the European Space Agency's (ESA) first European Remote Sensing (ERS-1) satellite, specifically, imagery from C-band (5.7 cm) microwave SAR. Among the algorithms for motion tracking in the Antarctic, the method by Drinkwater and Kottmeier [18] is one of the more successful ones. The data set obtained using their method from Ice Station Weddell (ISW) 1992 [16], [15] is the one we chose to validate our algorithm.

## 2. Relevant Background

Since the original description of the problem by Horn and Schunck in the seminal work [24], optic flow estimation has been a much researched topic. Under the assumption of extremely small temporal resolution the optic flow equation is considered valid and many techniques have been developed to estimate the flow field [25], [3], [5]. Robust techniques [8], [6], [36] have emerged to handle the large noise and/or the failure of the underlying image motion model.

Sequential pairs of SAR images capture two important characteristics of sea-ice motion, global translation and differential non-rigid dynamics. Due to differences in satellite orbits and the earth's rotation, the visual capture of local sea-ice dynamics is overshadowed by the complexity to ascertain high magnitude global translation (on the order of about 200 pixels on 100m resolution images separated in time by three (3) days). Traditionally this problem has been addressed using a hierarchical framework [11], [4]. Specifically within the field of sea ice, this problem is currently addressed using a variety of methods including cross correlation and 2D wavelets [21], [28], [29], [20], [16], [15], [31], [30].

An added complexity in this traditional methodology comes from the fact that high-spatial resolution SAR data is limited by low-temporal resolution due to polar orbital constraints (typically 3 days). Under the influence of fast moving storms, significant non-linear changes in discontinuities can occur at temporal scales much lesser than 3 days and sea ice can deform rapidly resulting in large changes in the orientation, distribution, and size of continuous and discontinuous regions. Thus estimation of the motion field in SAR imagery requires an added perspective when compared to the traditional optical flow algorithms. The hypothesis considered here is that motion can be extracted in a hierarchical fashion with coarse resolution levels resolving large global translation through linear models and finer resolution levels resolving smaller local non-rigid dynamics using higher order parametric motion models such as affine, quadratic, etc.

## 3. Motion Estimation Technique

In this paper, we use phase correlation as the technique to estimate sea-ice motion. Extensive studies on the phase correlation process for motion estimation have been provided in [40], [41]. Various image registration techniques using the Fourier Transform exist in current literature [12], [38], [32]. Alliney, et al. [2] estimate object motion under the constraint that the background does not undergo significant changes. Stone, et. al., [39], and Foroosh, et. al., [22] provide algorithms to perform subpixel image registration using the phase correlation technique. Phase correlation as described in research literature is derived from the Fourier Shift Theorem which is a specialization of the Affine Fourier Theorem as proposed by Bracewell [10].

The affine theorem describes the separation of the displacement vector and the affine coordinate matrix in the frequency domain. When handling the large motion, as obtained in the satellite imagery, the global translation components overshadow the differential affine motion parameters and thus the affine theorem has an immense potential in estimating the motion since the translation component can be estimated independent of the affine parameters.

The translational component can be extracted from within the correlation equation using "whitening" zero-phase FIR filters  $H_1 = |F(\mathbf{u})|^{-1}$  and  $H_2 = |G^*(\mathbf{u})|^{-1}$  [33] leading to a Dirac delta function centered at the translation parameters as in Eq. 1

$$\mathfrak{F}^{-1}\left(\frac{F(\mathbf{u})}{H_1} \frac{G^*(\mathbf{u})}{H_2}\right) = \delta(\mathbf{x} - \mathbf{d}) \quad (1)$$

The main advantage of phase-based techniques are its characteristic insensitivity to correlated and frequency-dependent noise. With the availability of the 2-D FFT [13], the calculations can be performed with much lower computational complexity. The disadvantage with these techniques is that they are applicable only under well-defined transformations and thus require bolstering from other techniques, especially in the cases where the transformations are arbitrary. A point of consideration is that phase correlation peak may reduce in height under image rotation and scaling [32]. For sea-ice SAR imagery, these can be assumed negligible since the global translation is large compared to affine parameters and thus not significantly affected by the magnitude reduction.

### 3.1. Processing Method

Global translations of sea ice in SAR imagery are of order 100 to 200 pixels depending on the temporal distance between images. The traditional method of "Normalized Cross Correlation" requires a large support window to

capture large translation but these large windows encompass a combination of various motions such that accuracy of the estimation procedure is limited to a spatial resolution much larger than the image resolution. Additionally, SAR is an active microwave system with an emitting signal in the range of centimeters (e.g., C-band has 5.7 cm wavelength). Materials like sea ice with crystalline features the same size as the emitted signal introduce considerable backscatter which, in turn, alters and blends the return signal between pixels. Phase correlation has the basic property of being illumination invariant and can therefore be used robustly to estimate the large motion at a low computational burden.

As a preprocessing step prior to the estimation, the ERS-1 images were modified using histogram equalization in tandem with mid-tone modification to obtain "visually significant regions" [7]. Experiments with various equalization methods indicated that the estimated motion field had the smallest error variance when mid tone expansion was applied.

To tackle the large translational motion, the motion field was estimated using a multi-resolution hierarchy of images obtained by decimating the image signal using a median filter. The median filter was used instead of a Gaussian filter because of the poor response of Gaussian Kernels in regions with heterogeneity, which constitute the differential features such as leads, families of slip lines, cracks, and ridges.

Each image resolution hierarchy obtained from an image pairs is used to estimate global motion by performing phase correlation at each level of the hierarchy and then passing that coarse estimate on as an initial estimate to the next finer level of the pyramid. The global motion is obtained at a particular level of the pyramid by binning the motion vectors at that level into a histogram. The histogram bucket containing the maximum number of candidates is taken as the estimate at that level of the hierarchy and submitted to the next level as the initial guess. This process is repeated down to the finest resolution image in the pyramid hierarchy where the final estimated solution is chosen as the global translation. To improve robustness of the method, potential median candidates at each level in the pyramid hierarchy are selected and passed through a "Lorentzian estimator" [9] to determine the best possible estimate.

Due to the periodic nature of the Discrete Fourier Transform, the maximum measurable estimate using the Fourier Transform of a signal within a window of size  $W$  is  $W/2$ . Thus, to capture translations of magnitude  $(u, v)$ , the window size should be at least  $2 * \max(u, v)$ . For the ERS-1 experimentation, the block size was taken as  $32 \times 32$  and the window size was taken as  $128 \times 128$ . The sizes of the window and the block are maintained constant throughout the entire pyramid hierarchy. This provided a method of obtaining accurate estimates at the coarsest level of the pyra-

mid which amplified to large translations at the finer scales of the image pyramid. Experience with ERS-1 SAR images shows that a three level pyramid ranging in resolutions from  $1536 \times 1536$  to  $384 \times 384$  is sufficient to capture the observed large translation.

Having obtained the global motion compensated image, a local piece-wise linear motion model is applied using phase correlation. This local motion model then provides two important pieces of information to the affine parametric model: (1) an initial estimate for the affine motion and (2) a correlation map.

For this experiment, the affine model chosen is a least-square regression technique. It is applied making use of a known limitation of correlation methods, namely, their inability to resolve regions of discontinuity [41]. Low values of correlation coefficient on the correlation map are thus used to isolate discontinuities so that the motion model can track the deformations in the vicinity of these long narrow crack-like features but avoid computations right at the discontinuities.

### 3.2. Validation Data Set

The European Space Agency's ERS - 1 and ERS - 2 C-band (5.3 GHz, 5.7 cm) Active Microwave Instrument are currently being used to generate weather independent (day or night), frequent repeat, high resolution (10 m) 100 km swath radar images globally and, in this particular case, for the Weddell Sea in the Southern Ocean around Antarctica. The 5 month Ice Station Weddell 1992 (ISW) is the only winter field experiment to date conducted in the Western Weddell Sea. The orbit phasing of the ERS - 1 was fixed in the 3-day exact repeating orbit called the "ice-phase" orbit providing uninterrupted SAR imagery of spatial coverage of  $100 \times 100 \text{ km}^2$  during the entire duration of the experiment.

The SAR images obtained from ERS -1 are projected onto the polar stereographic Special Sensor Microwave Imager (SSM/I) grid. The images are then block averaged to 100 m resolution ( $8 \times 8$  pixel block averaging) to speckle filter the images to minimize intensity errors to  $\pm 1 \text{ dB}$  ( $>90\%$  confidence interval) leading to images with dimensions of 1536 pixels in the horizontal and vertical direction.

Motion vectors for each  $100 \times 100 \text{ km}^2$  SAR image are resolved using a nested cross-correlation procedure [16], [15] to characterize  $5 \times 5 \text{ km}^2$  spatial patterns. A total of 11 such image pairs exist from this processing with an RMSE less than 0.5 cm/s for 3-day tracking compared against six buoy measurements from the ISW [16].

## 4. Results and Analysis

The global estimates obtained using our processing method are compared against the ISW results described in

Section 3.2. The global motion field used in the comparison is obtained by converting the motion field from pixel coordinates to the Special Sensor Microwave Imager (SSM/I) grid coordinates and plotting them in tandem with the ISW motion vectors.

To maximize the throughput of the FFT modules the phase correlation is performed on a window size with powers of 2. Depending on the spatial resolution required for the interpolation of the motion field, the block size can be adjusted at  $8 \times 8$ ,  $16 \times 16$  or  $32 \times 32$  leading to an output motion field at 0.8 km, 1.6 km or 3.2 km resolution.

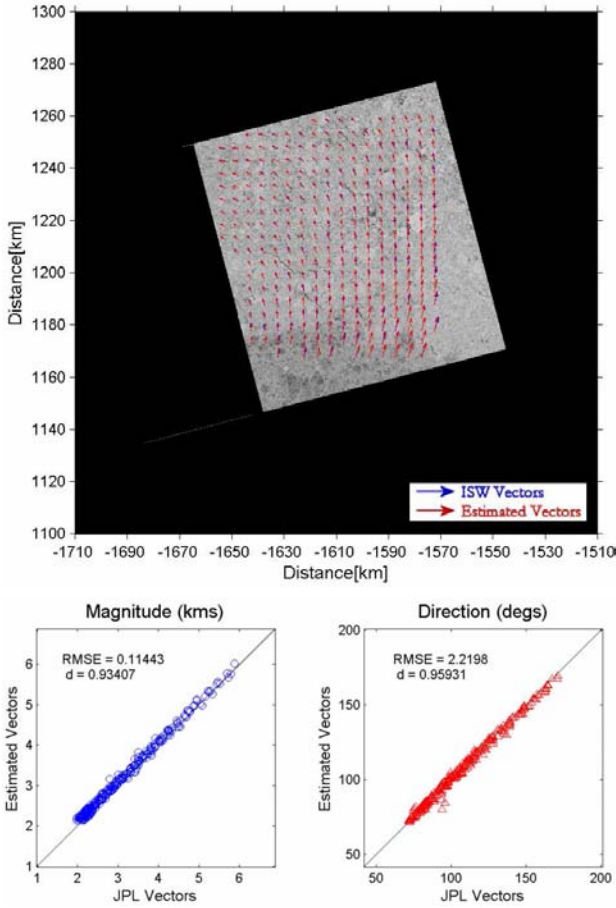


**Figure 1. Comparison of motion vectors from the ERS-1 image pair at orbit 3402 frame 5103 and orbit 3412 frame 5693 shown with our estimated vectors (red) and the ISW vectors (blue). Scatter plot comparisons of the magnitude and phase between these two data sets shown in accompanying panels.**

The subsequent results in Figure 1 show the accuracy of the estimates obtained by the phase correlation technique

in comparison with the ISW vectors. The estimated motion field in the images below have been computed using a  $32 \times 32$  window and then overlaid, using linear interpolation, on a 5 km SSM/I grid for comparison with the ISW vectors. Scatter plots show the magnitude and phase variation between our estimates and the ISW vectors for the spatially collocated positions.

Figure 1 is an illustrative example of the comparison between the ISW ground truth vectors (in blue) and the estimated vectors (in red). The bottom panel in Figure 1 shows scatter plots of the magnitude and directional components of the estimated vectors with the ISW vectors.

Two statistical measures of the similarity, the Root Mean Square Error (Eq. 2) and the index of agreement (Eq. 3) have been computed.

$$RMSE = \sqrt{\frac{1}{K} \sum_{k=1}^K (p_k - o_k)^2} \quad (2)$$

$$d_\gamma = 1 - \frac{\sum_{k=1}^K \omega_k (p_k - o_k)^\gamma}{\sum_{k=1}^K \omega_k (|p_k - \bar{o}| + |o_k - \bar{o}|)^\gamma} \quad (3)$$

where  $p_k$  are the predicted samples,  $o_k$  are the observed ground truth vectors,  $w_k$  are the weight functions which are assumed uniform for this study and  $\bar{o}$  is the mean of the observed data.  $\gamma$  is the order of index and according to Willmott [43],  $\gamma = 1$  is most robust for comparing results because of its linear approach to a perfect match.

Analysis of the image pairs using higher resolution analysis windows (Figure 2) reveals precise demarcations corresponding to the regions in the ice-flow undergoing significant amounts of non-rigid dynamics. Based on the variance of the magnitude and direction of the motion field, the cluster map as shown in Figure 2 was created using a quad-tree model.

This result reveals the usefulness of local higher order motion in the vicinity of the regions of discontinuity. Given the global motion compensated images, local non-rigid dynamics was first extracted using the simplest model of the local motion. Under the assumption that magnitude of the differential motion is small, a piecewise linear approximation of the non rigid motion using phase correlation was applied. As seen in Figure 3, the estimated local motion vectors are overlaid upon the correlation map to verify the goodness-of-fit as are the ISW vectors in validation. Experimentally, a threshold correlation of  $< 0.2$  is found to be the most appropriate for demarcating between continuous and discontinuous regimes. This low correlation corresponds to regions where the magnitude of deformation far exceeds the piece-wise approximation.

The dynamic region analyzed and described earlier in (Figure 2) is shown again in Figure 4 in the same format as Figure 3 for comparison. This dynamic region contains

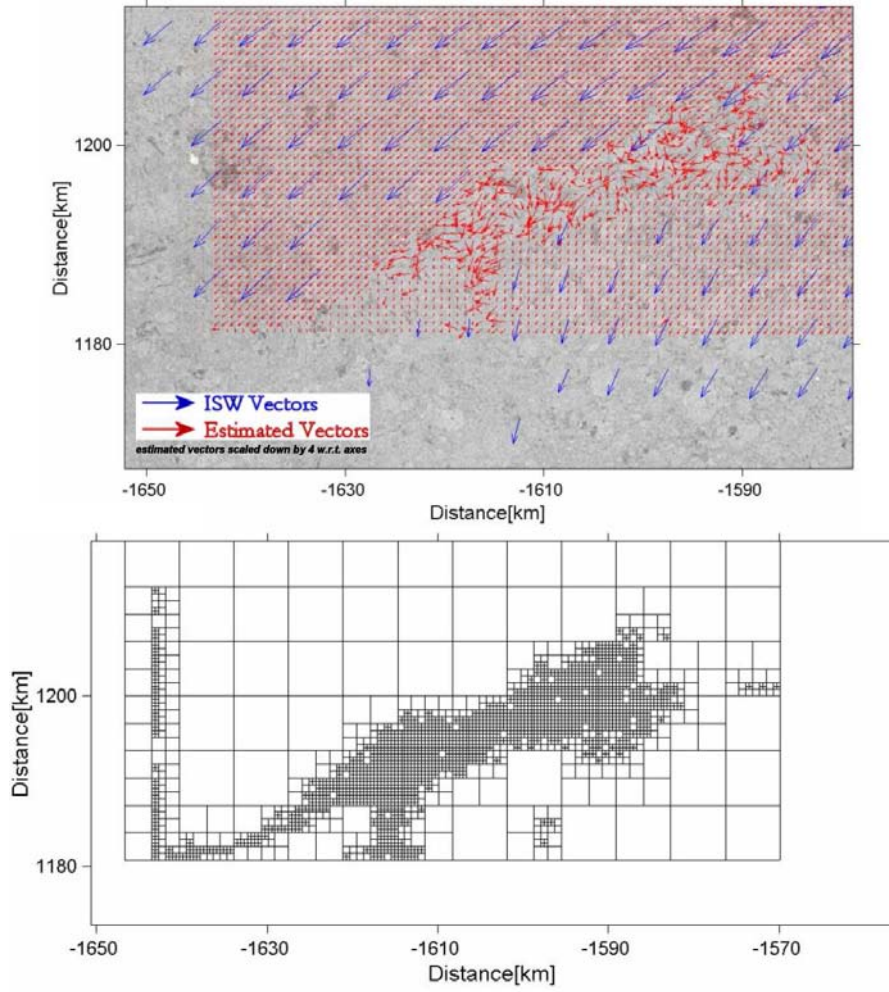


**Figure 2. Comparison between the estimated vectors and ISW vectors from the SAR image pair at orbit 3197 frame 5693 and orbit 3230 frame 5103 at a dynamic zone.**

lots of pixels without vector solutions because these pixels did not meet our correlation threshold. Such areas require a higher order model than our method currently includes. We note however, that the local motion is accurate in the high correlation regions as validated through comparison with the ISW vectors.

Due to the projection of the non linear components of the higher order motion, the local motion so estimated contains false discontinuities (i.e. false positives). These discontinuities occur due to abrupt changes in the frequency components between the two regions under consideration causing variations in the estimated vector field. To reduce the effect of these false discontinuities, sub-pixel motion interpolation was carried out using a cubic spline within a window around the result of the local phase correlation. This proce-

dure reduced the bands of discontinuities within the motion field and also estimated the motion field at a finer resolution around the peak of the local estimate but at the cost of increased computational complexity.

Figure 5 is the combined scatter map over all the image pairs used in this analysis. As can be seen, the majority of data points (estimated vectors) cluster along the one-one line with very small dispersion.  $n_{complete}$  is the total number of motion vectors and  $n_{good}$  are the points that are within 400 m (4 pixel) of the ISW vectors. This deviation is at the threshold of SAR geolocation accuracy [15] and therefore a scatter based on instrument accuracy rather than the technique applied.  $n_{deformation}$  are all the points in the correlation maps having low correlation. Thus 72.8% of the estimated motion vectors are accurate with respect

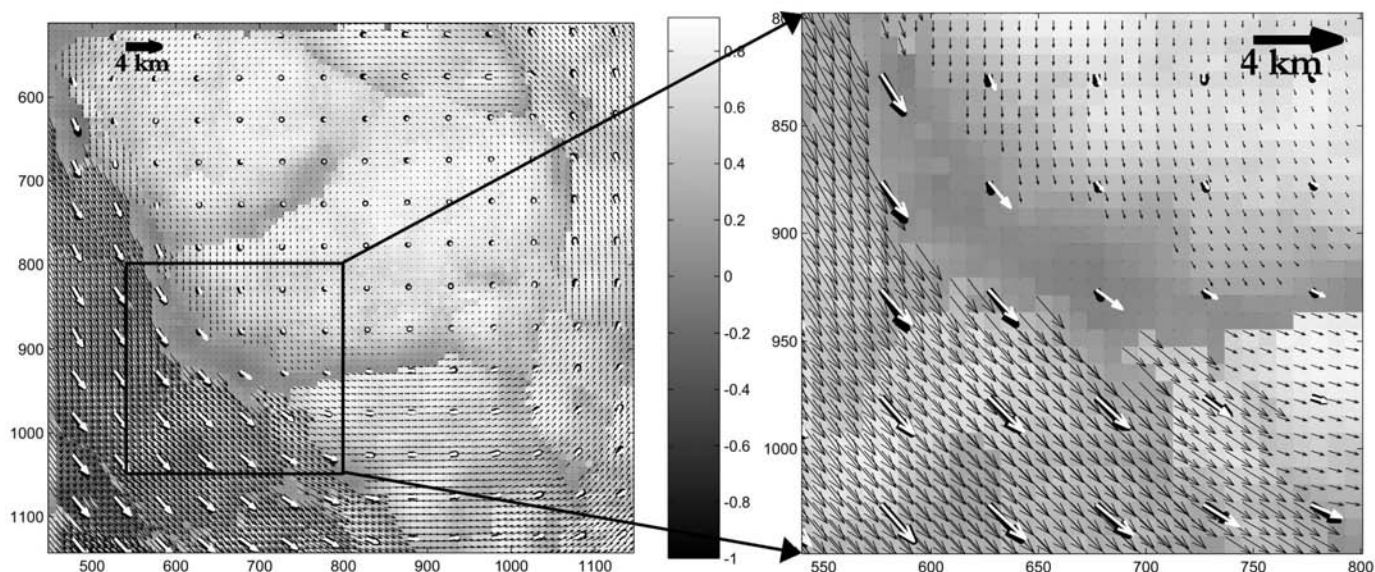


**Figure 3. Relative motion field between SAR image pair of orbit 3412 frame 5693 and orbit 3455 frame 5693 is shown. Grey-scale map plotted with lightest to darkest denoting high to low correlation coefficient with darkest defining discontinuity regions (without motion vectors) in the high resolution product (0.8 km resolution thin black vectors). Interpolated motion vectors at 5 km resolution (thick black) further superimposed with coincident ISW vectors (thick white) which hide nearly all of each thick black vector in validation.**

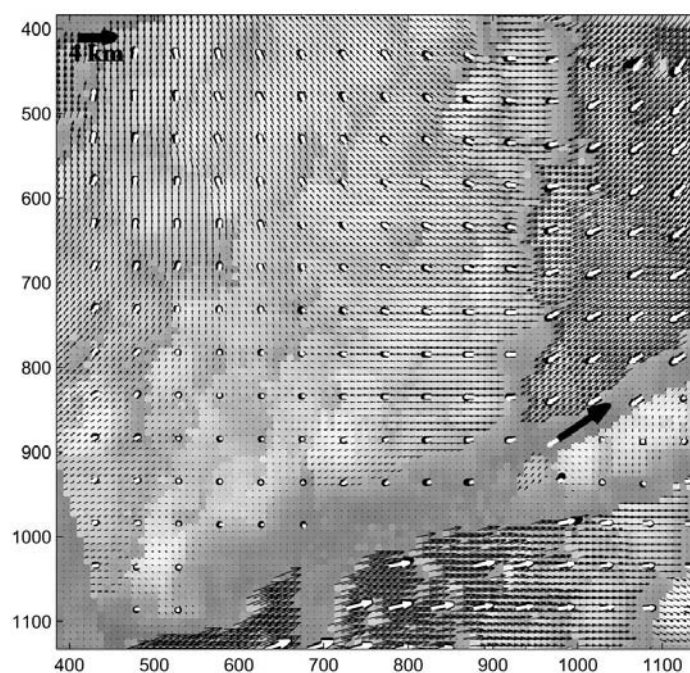


**Figure 4. Relative motion for SAR image pair with orbit 3197 frame 5693 and orbit 3230 frame 5103 showing the highly dynamic region presented in Figure 2 earlier.**

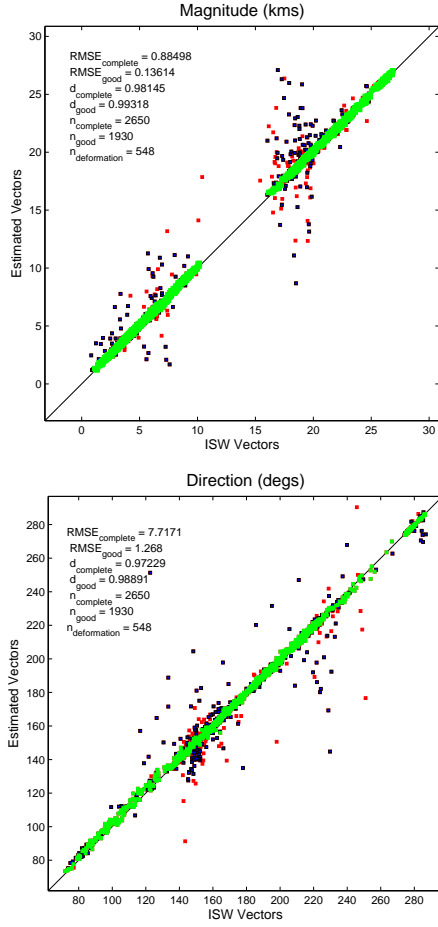


**Figure 5. Scatter plot of the estimated vectors v/s ISW vectors for the entire sequence of images during ISW. Green indicate the good points, blue are the deforming points and red are points we can not explain.**

to ISW vectors. Including flagged points undergoing deformation we can account for 93.5% of all the data points. The remaining 6.5% of data are displacement results greater than 400m which we can not account for using a correlation map. These points mainly correspond to regions where the gradient of the velocity is high and, in principle, requires a higher-order motion model to localize the position of the discontinuity accurately. Also indicated in the scatter plot are the RMSE (Eq. 2) and index of agreement (Eq. 3) for the complete data set and the “good” data set indicating a high accuracy between the ISW vectors and our estimated motion vectors.

To improve upon the estimated parameters, an affine motion is imposed onto the local piece-wise linear motion. This is performed specifically in the regions of discontinuity

as obtained from the correlation map. The affine parameter estimation chosen is a least-squares fit to the locally translated patch. The Peak Signal to Noise Ratio (PSNR) values, calculated using Eq. 4, are provided in Table 1.

$$PSNR = 20 * \log_{10} \left[ \frac{255}{\sigma_{|Image_1 - Image_2|}} \right] \quad (4)$$

where  $\sigma$  is the standard deviation,  $Image_1$  and  $Image_2$  is the image pair under consideration. From the table it is evident that the PSNR value between  $Image_2$  and the motion compensated images increases with increasing motion model complexity.

## 5. Conclusion

Localizing and parameterizing discontinuities is an important landmark for sea-ice research. Due to the low temporal resolution of the SAR images, this type of information is paramount input into numerical models for interpretation of events between SAR scenes. This paper describes a hierarchical method to estimate the parameters of a discontinuous motion field such as the ones captured by the ERS-1 SAR imagery in three stages. The hypothesis of using a finer sieve to filter out coarse motion models iteratively seems to be validated with the observed improvement in the PSNR values of the motion compensated images.

The comparative results between the estimated vectors and the ISW ground truth vectors indicate that hierarchical phase correlation is ideal for the estimation of the global motion. This is mainly due to the inherent robustness of phase correlation to illumination variation and its ability to capture large translational components without getting caught in local minima. Additionally, the usage of the Fast Fourier Transform in the calculation of the phase correlation term makes the computation significantly faster than optic flow methods.

The second stage involves isolation of discontinuous regions using local piecewise linear model followed by the third stage of estimating affine parameters along regions of discontinuities. Under the assumption that the net motion is actually composed of a large global motion component and small local deformations, this method captures the large global motion component and the local deformation using an affine motion model.

As a subsequent stage to the current research, the estimate of the local deformation could be improved using robust parameter estimation techniques and also inclusion of a motion model such as the quadratic. Another possible track for future research would be a feature-based approach in tandem with global motion estimation in order to improve the overall robustness of the estimated global motion.

## 6. Acknowledgments

The ERS-1 SAR images and associated tracked ice motion vectors were provided courtesy of Mark Drinkwater to advance the rendering of sea-ice motion products of Antarctic sea ice as started under NSF OPP-9818645. ERS-1 scatterometer images were originally processed by David Long of Brigham Young University as part of the collaborative ESA-supported AO2.USA.119 project: SAR data were also supplied courtesy of ESA, 1992, and processed to ice motion under the same study. Further development of a motion tracking algorithm was made possible through ONR N00014-03-1-0045 and N00014-02-1-0244.

**Table 1. Comparison of PSNR between motion compensated images and Image<sub>2</sub>, PSNR<sub>G</sub> - Global, PSNR<sub>LL</sub> - Local Linear, PSNR<sub>LA</sub> - Local Affine**

Image <sub>1</sub>	Image <sub>2</sub>	PSNR <sub>G</sub>	PSNR <sub>LL</sub>	PSNR <sub>LA</sub>
2982-5693	3025-5693	13.109	13.934	14.116
3058-5103	3068-5693	13.915	14.834	15.006
3068-5693	3111-5693	14.865	16.135	16.477
3111-5693	3144-5103	11.419	11.611	11.649
3144-5103	3154-5693	14.128	15.268	15.414
3154-5693	3197-5693	11.351	11.395	11.379
3197-5693	3230-5103	15.715	18.538	19.080
3230-5103	3283-5693	14.213	15.645	15.947
3402-5103	3412-5693	12.489	13.944	14.078
3412-5693	3455-5693	12.850	13.645	13.689
3412-5713	3455-5713	13.446	14.524	14.699

## References

- [1] Y. Aksenov and W. D. H. III. Failure propagation effects in an anisotropic sea-ice dynamics model. In J. Dempsey and H. Shen, editors, *IUTAM Symposium on Scaling Laws in Ice Mechanics and Ice Dynamics*, pages 363–372, Netherlands, 2001. Kluwer Academic Publishers.
- [2] S. Alliney, G. Cortelazzo, and G. Mian. On the registration of an object translating on a static background. *Pattern Recognition*, 29(1):131–141, 1996.
- [3] P. Anandan. *Measuring Visual Motion from Image Sequences*. PhD thesis, University of Massachusetts, 1987.
- [4] P. Anandan. A computational framework and an algorithm for the measurement of visual motion. *International Journal of Computer Vision*, 2(3):283–310, January 1989.
- [5] P. Anandan, J. R. Bergen, K. J. Hanna, and R. Hingorani. Hierarchical model-based motion estimation. In *Proceedings of European Conference on Computer Vision*, pages 237–252, 1992.
- [6] A. Bab-Hadiashar and D. Suter. Robust total least squares based optic flow computation. In *ACCV*, pages 566–573, 1998.
- [7] S. Bhukhanwala and T. V. Ramabadran. Automated global enhancement of digitized photographs. *IEEE Transactions on Consumer Electronics*, 40(1):272 – 278, February 1994.
- [8] M. Black and P. Anandan. A framework for the robust estimation of optical flow. In *Proceedings of IEEE Computer Society International Conference on Computer Vision*, pages 231–236, 1993.
- [9] M. J. Black. *Robust incremental optical flow*. PhD thesis, Yale University, 1992.
- [10] R. N. Bracewell, K.-Y. Chang, A. K. Jha, and Y.-H. Wang. Affine Theorem for two-dimensional Fourier Transform. *Electronics Letters*, 29(3):304, February 1993.
- [11] P. J. Burt and E. H. Adelson. The laplacian pyramid as a compact image code. *IEEE Transactions on Communications*, COM-31,4:532–540, 1983.
- [12] E. D. Castro and C. Morandi. Registration of translated and rotated images using finite fourier transform. *IEEE Transactions on Pattern Analysis and Machine Intelligence*, 9:700–703, 1987.
- [13] J. W. Cooley and J. W. Tukey. An algorithm for the machine calculation of complex fourier series. *Math. Comput.*, 19:297 – 301, April 1965.
- [14] M. D. Coon, G. S. Knoke, D. C. Echert, and R. S. Pritchard. The architecture of an anisotropic elastic-plastic sea ice mechanics constitutive law. *J. of Geophys. Res.*, 103(C10):21915–21925, September 15 1998.
- [15] M. Drinkwater. *Analysis of SAR Data of the Polar Oceans*, chapter Satellite microwave radar observations of Antarctic sea ice, pages 145–187. Springer-Verlag, 1998.
- [16] M. Drinkwater. *Antarctic Sea Ice: Physical Processes, Interactions, and Variability*, volume 74, chapter Active microwave remote sensing observations of Weddell sea ice, pages 187–212. Antarctic Research Series, 1998.
- [17] M. R. Drinkwater. Recent advances in radar remote sensing. In *newsletter of the SCAR Global Change Programme*, volume 1, 1996.
- [18] M. R. Drinkwater and C. Kottmeier. Proc. IGARSS '94. In *Satellite microwave radar- and buoy-tracked ice motion in the Weddell Sea during WWGS '92*, volume 1, pages 153–155, Pasadena, CA, August 1994.
- [19] M. R. Drinkwater and X. Liu. ERS satellite microwave radar observations of antarctic sea-ice dynamics. In *Proc. 3rd ERS Scientific Symposium*, Florence, Italy, 1997.
- [20] W. J. Emery, C. Fowler, J. Hawkins, and R. Preller. Fram Strait satellite image-derived ice motions. *Journal of Geophysical Research*, 96 (C5):8917–8920, 1991.
- [21] M. Fily and D. A. Rothrock. Sea-ice tracking by nested correlations. *IEEE Trans. Geosci. Remote Sens.*, GE-25(5):570–580, 1987.
- [22] H. Foroosh, J. B. Zerubia, and M. Berthod. Extension of phase correlation to subpixel registration. *IP*, 11(3):188–200, March 2002.
- [23] M. A. Hopkins. A discrete element lagrangian sea-ice model. to appear in *J. Engineering Computations*, in press.
- [24] B. Horn and B. Schunck. Determining optical flow. *Artificial Intelligence*, 17:185–203, 1981.
- [25] J. R. Jain and A. K. Jain. Displacement measurement and its application in inter-frame image coding. *IEEE Transactions on Communication*, 29:1799 – 1806, December 1981.

- [26] C. Kambhamettu, D. B. Goldgof, D. Terzopoulos, and T. S. Huang. Nonrigid motion analysis. In T. Y. Young, editor, *Handbook of Pattern Recognition and Image Processing: Computer Vision*, pages 405–430, 1994.
- [27] R. Kwok. Deformation of the arctic ocean sea ice cover between november 1996 and april 1997: A qualitative survey. In J. Dempsey and H. Shen, editors, *IUTAM Symposium on Scaling Laws in Ice Mechanics and Ice Dynamics*, pages 315–322, Netherlands, 2001. Kluwer Academic Publishers.
- [28] R. Kwok, J. C. Curlander, R. McConnell, and S. Pang. An ice motion tracking system at the alaska SAR facility. *IEEE J. Oceanic Eng.*, 15(1):44–54, 1990.
- [29] R. Kwok, A. Schweiger, D. A. Rothrock, S. Pang, and C. Kottmeier. Sea-ice motion from satellite passive microwave imagery assessed with ERS SAR and buoy motions. *Journal of Geophysical Research*, 103 (C4):8191–8214, 1998.
- [30] S. Li, Z. Cheng, and W. F. Weeks. *Analysis of SAR Data of the Polar Oceans*, chapter Extraction of intermediate scale sea ice deformation parameters from SAR ice motion products, pages 69–90. Springer-Verlag, New York, 1998.
- [31] A. K. Liu and D. J. Cavalieri. On sea-ice drift from the wavelet analysis of the defense meteorological satellite program (DMSP) special sensor microwave imager (SSM/I) data. *Int. J. Remote Sens.*, 19(7):1415–1423, 1998.
- [32] L. Lucchese. A frequency domain technique based on energy radial projections for robust estimation of global 2D affine transformations. *Comput. Vis. Image Underst.*, 81(1):72–116, 2001.
- [33] R. Manduchi and G. A. Mian. Accuracy analysis for correlation-based image registration algorithms. In *ISCAS*, pages 834–837, 1993.
- [34] S. L. McNutt and J. E. Overland. Considerations of scale and hierarchy in remote sensing of sea ice in the Beaufort, Chukchi, and Bering Seas. In *International Glaciology Symposium*, Fairbanks, Alaska, 2000.
- [35] R. E. Moritz and H. L. Stern. Relationships between geostrophic winds, ice strain rates and the piecewise rigid motions of pack ice. In J. Dempsey and H. Shen, editors, *IUTAM Symposium on Scaling Laws in Ice Mechanics and Ice Dynamics*, pages 335–348, Netherlands, 2001. Kluwer Academic Publishers.
- [36] E. P. Ong and M. Spann. Robust optical flow computation based on least-median-of-squares regression. *Int. J. Comput. Vision*, 31(1):51–82, 1999.
- [37] J. E. Overland, S. L. McNutt, S. Salo, J. Groves, and S. Li. Arctic sea ice as a granular plastic. *Journal of Geophysical Research*, 103:21845–21868, 1998.
- [38] B. Reddy and B. Chatterji. An FFT-based technique for translation, rotation, and scale-invariant image registration. *IEEE Trans. Image Processing*, 5:1266–1271, August 1996.
- [39] H. S. Stone, M. T. Orchard, E. C. Chang, and S. A. Martucci. A fast direct Fourier-based algorithm for subpixel registration of images. *GeoRS*, 39(10):2235–2243, October 2001.
- [40] G. A. Thomas. Television motion measurement for datv and other applications. Technical report, BBC Research Department, 1987.
- [41] D. Vernon. *Fourier Vision - Segmentation and Velocity Measurement using Fourier Transform*. Kluwer Academic Publishers, 2001.
- [42] A. V. Wilchinsky and D. L. Feltham. A continuum anisotropic model of sea ice dynamics. *Journal of the Royal Society*, 2004. in press.
- [43] C. J. Willmot, S. G. Ackleson, R. E. Davis, J. J. Feddema, K. M. Klink, D. R. Legates, J. O’Donnell, and C. M. Rowe. Statistics for the evaluation and comparison of models. *Journal of Geophysical Research*, 90:8995 – 9005, 1985.